International Journal of Fluid Power 8 (2007) No. 2 pp. 47-62

HYDROSTATIC HYBRID SYSTEM: SYSTEM DEFINITION AND APPLICATION

Alarico Macor and Marco Tramontan

Dipartimento di Tecnica e Gestione dei Sistemi Industriali, Università di Padova, Sede di Vicenza, Stradella S. Nicola, 3 - 36100 Vicenza, Italy
alarico.macor@unipd.it

Abstract

The use of high efficiency engines is an unavoidable necessity in the transportation field. The reduction of gas emissions and the optimisation of conversion efficiency cannot be entrusted only to engine characteristics, but it is necessary to work with integrated propulsion systems, which have to manage the production and transmission of the energy in an optimal way. In this paper a hybrid propulsion system made of a parallel type hybrid engine and a hydrostatic transmission is presented. The operational flexibility of the hydrostatic transmission allows the thermal engine to operate at a constant speed, hence at maximum efficiency and/or minimum emission conditions. This propulsion system was applied to the case of a "12 m class" bus for passenger transportation. An Italian hybrid vehicle was taken as the reference solution for performance comparison and as a technical database for the vehicle design aid. Starting from the Italian laws regarding buses, the design and sizing of the propulsion group components were performed. Then, in order to verify the ability of the hybrid scheme to satisfy the design targets, a simulation of the system was carried out using a dynamic simulation code. The simulation showed that the combination of the hydrostatic transmission with the hybrid engine leads to energy savings and a pollutant reduction in comparison with the reference vehicle.

Keywords: vehicular hybrid propulsion, hydrostatic transmission

1 Introduction

Environmental and economical issues today are making it necessary to develop efficient, clean, and sustainable solutions for transportation. The performance and environmental impact of traditional diesel and spark ignition engines are continuously being improved, and, in recent times, new kinds of propulsion have emerged: electric vehicles, electric hybrid vehicles, and hydrogen vehicles. Hybrid electric vehicles are currently considered the most viable alternative propulsion system, also as a base for the future technology of fuel cells (Bitsche et al., 2004, Maggetto et al., 2001).

A hybrid propulsion system uses two different energy sources, a thermal engine and an electrical motor, acting together in order to satisfy the required performance, better exploiting fuel. In traditional thermal propulsion units, the maximum power required by the engine for the accelerations is much greater than the average power (3-6 times); this forces the engine to run at power levels close to the maximum for short periods leaving it running at partial loads and low efficiency for the remaining time. A solution to this problem could be the adoption of a small engine, in theory having a power equal to the average required power, and a storage energy system for accumulating the energy surplus produced by the engine in the periods of low load; this system would give back the energy previously stored during the peak phases. In electric hybrid systems this job is accomplished by an electric apparatus.

The components of a hybrid system can be assembled in several architectures, which are categorized as series, parallel or series-parallel schemes, engine or battery dominant, charge sustaining or charge depleting. An exhaustive review of them can be found in Miller (2004). The three main types will be now briefly illustrated.

In series hybrid systems (Fig. 1a) only the electric motor (EM) provides the propulsion power; the internal combustion engine (ICE) drives the electric generator (EG) to produce an electrical current that can directly be used by the EM, or stored in the battery. During start-up or acceleration, both the ICE and battery de-

This manuscript was received on 3 September 2004 and was accepted after revision for publication on 6 June 2007

liver electrical energy to the EM; during braking, the EM acts as a generator, since it is driven by the inertia force, and converts the vehicle's kinetic energy into electrical energy storing it in the battery (regenerative braking).

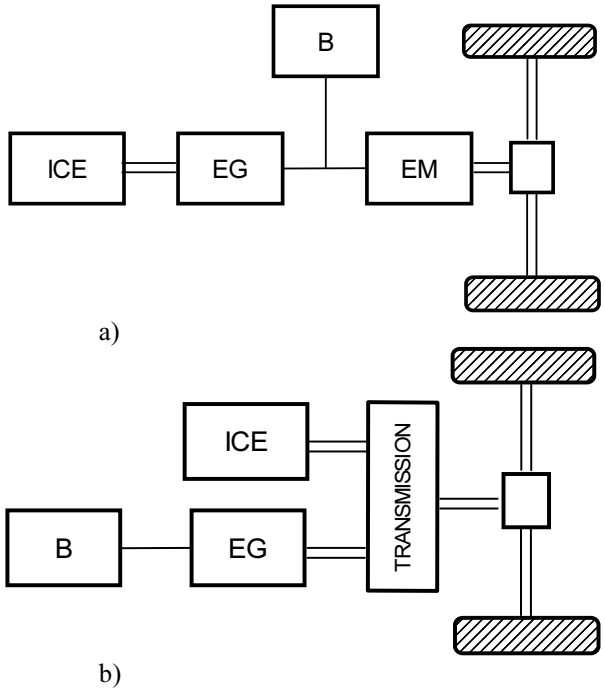

Fig. 1: *Series (a) and parallel (b) hybrid systems*

Since the ICE is disconnected from the wheels, it can be set for its best operating range; moreover, it can be downsized to the average operating power. However, it requires a high number of components and regulators, and during braking the storage battery is heavily stressed by the EM, which is sized for the maximum traction power.

In parallel hybrid systems (Fig. 1b), both the ICE and the EM deliver power to drive the wheels: in this way they can be downsized. Regenerative braking is still possible, and with respect to a series system, there are fewer components and less energy flow conversion; on the other hand, the power blending from the ICE and EM requires a complex mechanical transmission and a complex control system.

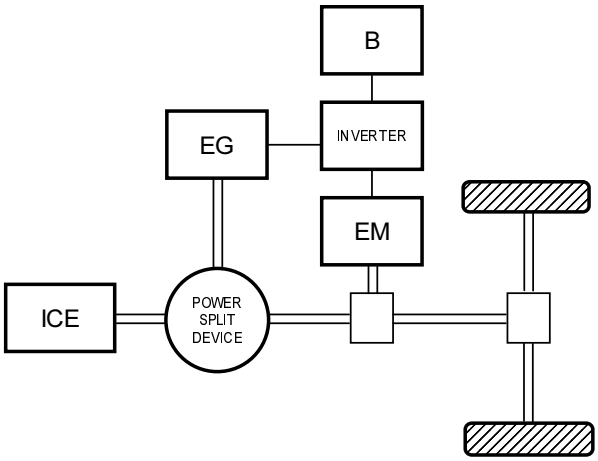

Fig. 2: *Series -parallel hybrid system*

In a series-parallel configuration, a small series element is added to a parallel structure (Fig. 2). Depending on the driving conditions, a power split device allocates the ICE power to the wheels and the EG. The power from the EG is delivered to the battery and/or EM, which operates in parallel to the ICE. This configuration includes the advantageous features of both series and parallel schemes, but it is relatively complicated and costly.

Many hybrid models are available today in the automobile market, the most well-known of which is the Toyota Prius, whose propulsion system is series-parallel system (55 kW Atkinson cycle ICE, 30 kW EM, power split transmission, nickel-metal hydride storage battery); its main competitor is the Honda Insight, a pure parallel scheme (50 kW ICE, 10 kW EM, manual or continuously variable transmission, nickel-metal hydride storage battery).

A series scheme is preferred on heavy vehicles, such as buses and trucks, even though applications on light vehicles can be found as well, such as FIAT's small Ecopower system.

In this work the discussion will be limited to public transport vehicles.

Hybrid buses have demonstrated to have great potential in fuel economy (*fe*) increase and emissions reduction.

The Northeast Advanced Vehicle Consortium (2000) summarized the performance of two hybrid series buses and a conventional 40-foot class diesel bus carried out on a heavy-duty vehicle chassis dynamometer following some standard test cycles. The hybrid buses showed higher *fe* and lower emission levels. For example, on a CBD14 test cycle, the hybrid buses showed *fe*=1.65 and 1.81 km/l, the diesel buses 1.48 km/l, and the average emission reductions of the hybrid buses were -36% NO, -50% PM, -99% CO.

Scott Wayne et al. (2004), testing a hybrid series bus and a conventional diesel bus on the chassis dynamometer, also found strong emissions reduction for hybrids (-50% NOx, -70%CO, -98% HC), but *fe* nearly the same as, and for some cycles also less then, the diesel bus, showing values ranging from 1.4 a 3.1 km/l.

Two similar experiments have been carried out during the last 10 years in Italy. The first one was the FLEETS project, sponsored by the European Union and carried out in Terni (Conti et al., 2000, Jefferson et al., 2002): the bus was a hybrid series type having a 30 kW ICE, 128 kW EM, lead-acid battery; its range is 30 km with electric drive and 250 km with a full tank. The annual distance covered by the bus was 40,000 km, compared to 90,000 km for traditional vehicles; the more frequent failures were located in the battery. The fuel consumption was nearly the same as for traditional buses, but the emissions were noticeably lower: HC -28%, CO -94%, NOX –50%. The second experiment took place in Genoa (Pini Prato et al., 2000). Synthetically: the vehicle, called Altrobus, was a series type, with a 30 kW diesel engine, 120 kW electric motor, Pb-acid battery; its fuel consumption was 20% lower than diesel fuelled buses and emissions were HC –89%, CO –82%, NOX –70%, particulate –90%.

The fuel economy of a vehicle *fe*, i.e. the distance covered per unit volume of fuel, can be expressed as:

$$fe = \frac{d}{V_u} = \frac{d\,\rho_f H_u}{E_{trac}}\eta \quad (1)$$

Fuel economy, *fe* does not depend only on the propulsion apparatus efficiency η, but also on the energy required for traction, E_{trac}. The efficiency η depends on the engine, transmission, and storage system efficiency, which must be as high as possible. The traction energy mainly depends on the rolling resistance and inertia force which, in turn, depends on the vehicle mass. So, to reduce the vehicle mass, smaller engines and lighter batteries must be used (the chassis can be considered as independent from propulsion system).

O'Keefe et al. (2002) analytically investigated the *fe* increase obtained by introducing some technology additions to a base series hybrid bus: a 30% reduction in the total vehicle mass led to a 0.38 km/l increase in the *fe* starting from a base value equal to 1.81 km/l; the downsizing of the ICE from 172 kW to 38 kW led to a 0.68 km/l increase; a 50% reduction in the battery mass (from 1500 kg to 700 kg) led to a 0.14 km/l gain. All the cases are very promising.

In a hybrid series bus, the battery is very heavy, mainly because of the long periods of time it must spend in "only electric" mode. Furthermore, the most commonly used battery type, lead-acid, has low energy density and allows very limited energy discharge. All this makes it necessary to oversize the battery. The Pb-acid battery, however, is the most reliable type because it tolerates the current peaks that occur during regenerative braking. To adopt a lighter battery, it is necessary to preserve it from peak currents. In other words, the electric motor must be downsized and run if possible at a constant speed.

In this work a parallel hybrid scheme with a hydrostatic transmission (HT) is proposed (Tramontan et al., 2002). The scheme tries to attain an increase in *fe* by means of a reduction in ICE size, an optimal management of the ICE and a reduction of the battery weight. The ICE is downsized to the average power and, thanks to the HT, kept at a constant speed, which can be chosen equal to that of minimum consumption or minimum emission. The battery feeds an asynchronous EM through an inverter. A control system acts on the displacements of the HT to vary the vehicle's speed. By checking the slip of the EM, overload at starting and at regenerative braking is avoided making it possible to use a lighter battery.

Other types of transmissions, such as a belt continuous variable transmission (Huang et al., 2004), a toroidal variator (torotrack), or a power split drive (Mikeska et al., 2002), and other types of energy storage systems, such as a litium-ion battery for its high efficiency, battery plus supercapacitors, or flywheels (Jefferson et al., 2002; Miller, 2004; Gulia et al., 2001) could be used. However, less expensive solutions using current technologies were preferred here, even if sometimes they may prove to be less efficient; more sophisticated technologies, when available, will certainly bring further benefits.

In this paper, the criteria for the design of the main components of this system and their application to an urban bus of the "12 m" class will be discussed. In order to verify the capability of the hybrid scheme to assure the design targets, a simulation of the hybrid engine-vehicle system was carried out using the code ITIsim (ITIsim 3.3, 2003), which makes it possible to perform a dynamic simulation of the fluid power and mechanical systems. The input conditions of the system model were both standard and real operating curves.

2 Hydrostatic Hybrid System

In heavy vehicle design, the choice between series and parallel configuration is conditioned by some factors: the main use of the vehicle, the required performance, the vehicle mass, reliability, and cost. These factors, which are often conflicting, must be combined in order to maximize the *fe*.

The main use of vehicles in urban transport involves many stops and gos and they must run for a long time. Therefore, the most commonly used hybrid configuration is a charge sustaining one with a series scheme.

The need to run for a long time in "only electric" conditions makes it necessary to adopt a large battery. The most commonly used battery in hybrid vehicles, the Pb-acid, has low energy density and, to guarantee an acceptable life, a small depth of discharge, nearly 20%. So the battery size must be at least 5 times that required simply for energy storage. On the other hand, this large mass is positive with regards to the reliability of the battery (which remains a weak point of all battery types): a large mass better absorbs the high current peaks that the EM sends to the battery during regenerative braking. It is worth remembering that the EM in a series scheme is sized for maximum traction power.

Hence, a strong reduction in battery mass without loss in reliability requires the reduction in the EM/EG size: this can be done, as previously shown, also in the parallel scheme, where, moreover, there is one less electric machine. However, the speed of the two motors isn't constant, as in series scheme, so the ICE cannot be set for its best operating range. To obtain this feature the parallel scheme could be combined with a hydrostatic transmission, which detaches the propulsion system from the traction wheels allowing the motors to run at a constant speed, equal to that of the minimum specific consumption or minimum emission level. The ICE size can be lowered, in theory down to average required power, allowing the engine to work closer to optimal conditions. Due to the small size and constant speed of the EM, fewer power peaks are produced during regenerative braking allowing the designer to adopt batteries with higher energy and power density such as a Nickel metal hydride (NiMH) battery. The NiMH battery shows a higher depth of discharge, 50%, so that the battery will be only two times larger than that required for a certain amount of energy storage. A NiMH battery is more delicate than a Pb-acid battery, and the reduced mass of a NiMH could make it less

resistant to current peaks: the constant speed of the EM and its reduced power should be a guarantee against this risk.

The advantages of HTs are well known: they allow for continuous speed variation simply by changing displacements; they operate over a wide range of torque/speed ratios; they can transmit high power with low inertia, and can reverse their operation making regenerative braking possible. Moreover, they can easily be protected against pressure peaks by means of relief valves; this feature is particularly important in this application where power peaks are to be avoided. Its drawback is efficiency, since in an HT a double energy conversion takes place: the efficiency can reach 0.83-0.85, but for low pressures, speeds and displacements the efficiency decreases; as a comparison, a mechanical transmission will typically have an efficiency of 0.95 or greater. This gap can be partly offset by suitably designing the HT so that the two hydraulic machines are calculated for work at maximum displacements, hence with high efficiencies, in the most frequent velocity range of the vehicle.

The scheme of the proposed system, called hydrostatic hybrid system (HHS) in this paper, is shown in Fig. 3. The ICE and EM are coupled on a single shaft and rotates close to the synchronous speed of the EM. A gearbox changes the engine speed into a correct speed for the HT; this component, of course, can be omitted when these speeds are close to each other. The EM is supplied by an inverter, which transforms the direct current coming from the storage battery in alternate current, without variations in frequency.

Two operating conditions are possible:

$P_{trac} > P_{ICE}$: the slip is positive; the EM operates as a motor and supplies P_{trac} - P_{ICE} to the traction absorbing it from the storage battery;

$P_{trac} < P_{ICE}$: the slip is negative; the ICE operates as a generator to supply P_{ICE} - P_{trac} to the storage battery.

Variations in the HT speed are made by the control system, which, depending on the driving requirements, changes the pump and motor displacements. During braking, the control system acts on the displacements reversing the HT operation; the EM becomes a generator and charges the battery, partly recovering the kinetic energy of the vehicle. When strong braking is required, the traditional braking system will operate.

The torque transmitted to the wheels and the torque received from the wheels during regenerative braking cannot exceed a maximum value: the limitation is carried out by the control system which checks the EM slip and changes the displacements keeping it within its linearity range. In this way the battery is never exposed to dangerous power peaks.

In the following paragraphs the main design criteria for the components of the hydrostatic hybrid system will be briefly discussed.

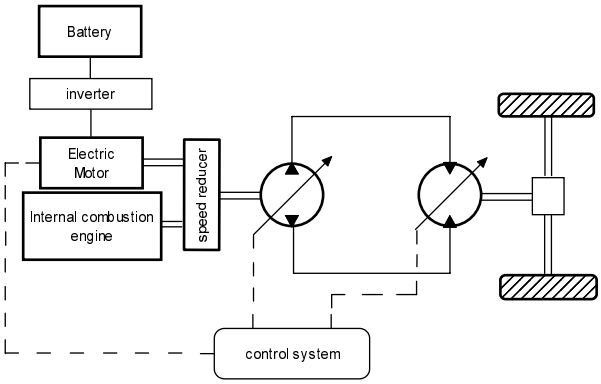

Fig. 3: *Scheme of the hydrostatic hybrid system*

2.1 The Internal Combustion Engine

As previously stated, the power to be supplied by the ICE is equal to, or slightly greater than, the average power required by the vehicle, which is much lower than the maximum one.

The average power can be estimated starting from the data of a vehicle having similar size as the vehicle in consideration: the fuel economy *fe* (km/l), the average speed $\overline{v}$ (km/h), and the average value for the specific fuel consumption of the engine $\overline{c}_s$. So, the average required power is:

$$\overline{P}_{req} = \frac{\overline{v}\rho}{\overline{c}_s \, fe} \tag{2}$$

The maximum power of the engine being chosen P_{ICE} shouldn't be too far from $\overline{P}_{req}$, otherwise we again end up over sizing. Finally, the engine speed must be selected according to the speed of the electric motor in the range of the minimum specific fuel consumption.

The absence of transients leads to beneficial effects on emissions, especially for particulate matter.

2.2 Electric Drive

The asynchronous electric unit must have a peak power equal to the difference between the maximum required power and the power supplied by the ICE:

$$P_{EMp} = P_{max} - P_{ICE} \tag{3}$$

No particular requirements must be fulfilled by this unit, except for efficiency, weight and compactness. Concerning these aspects, families of electric motors specially studied for vehicular traction having very low weights and volumes are available today in the market.

2.3 The Hydrostatic Transmission

In Fig. 4 the typical scheme of a hydrostatic transmission having a variable displacement pump and motor is shown; in Fig. 5 its torque-speed curve at maximum power is shown.

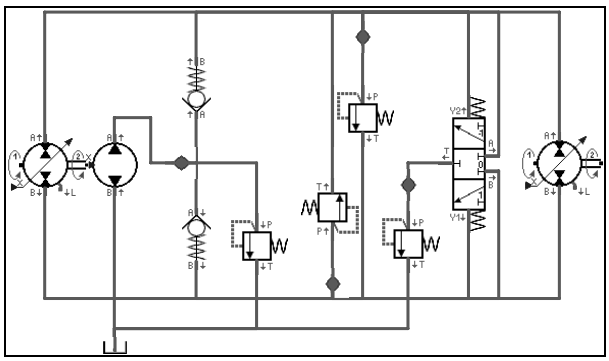

Fig. 4: *Scheme of a hydrostatic transmission*

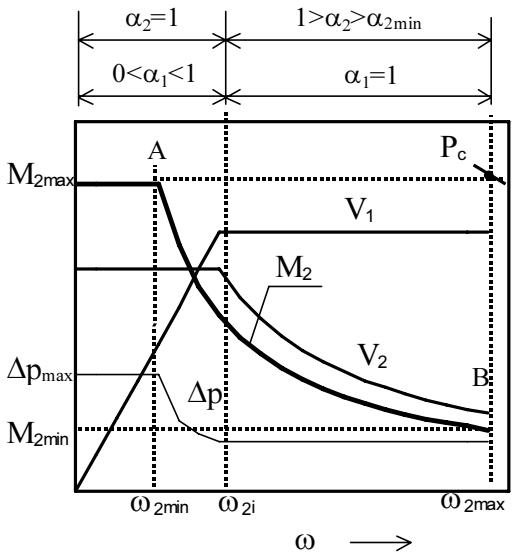

Fig. 5: *Torque-speed curve at maximum power of a hydrostatic transmission*

The torque-speed curve is bisected: in section one, to increase the output speed ω_2 the pump displacement is increased up to its maximum value, keeping the motor displacement at maximum value. In the second section the opposite happens: the motor displacement is reduced down to its minimum value, keeping the pump displacement at a maximum value.

The main problems posed by HT design are the calculation of the pump and motor displacement, and the regulation criteria to be adopted.

As far as the regulation criteria are concerned, the conversion range R must be calculated. R is the ratio between the corner power P_c, i.e. the product of the maximum torque and the maximum speed of the motor, and the maximum power of the hydraulic motor P_{2max} (Fig. 5) (Nervegna, 2000)1

$$R = \frac{P_c}{P_{2\max}} = \frac{M_{2\max}\omega_{2\max}}{P_{2\max}} \tag{4}$$

For the configuration at hand:

$$P_c = \frac{F_{\max} v_{\max}}{\eta_{g2}} \tag{5}$$

$$P_{2\max} = P_{he}\eta_{g1}\eta_{ht} \tag{6}$$

In the previous equations :
ω_{2max} is linked to v_{max} by the final ratio i_g and the wheel radius r:

$$\omega_{2\max} = \frac{v_{\max}}{r} i_g \tag{7}$$

P_{he} is the maximum power supplied by the hybrid engine.

In this way R can be calculated by:

$$R = \frac{F_{\max} \quad v_{\max}}{P_{he}\eta_{g1}\eta_{ht}\eta_{g2}} \tag{8}$$

On the other hand, R can also be written as (Fig. 5):

$$R = \frac{M_{2\max}\omega_{2\max}}{M_{2\max}\omega_{2\min}} = \frac{\omega_{2\max}}{\omega_{2\min}} \tag{9}$$

The generic angular velocity ω_2 can be derived equating the pump and motor flow rate:

$$\omega_2 = \omega_1 \frac{\alpha_1 V_{1\max}}{\alpha_2 V_{2\max}} \eta_{v1}\eta_{v2} \tag{10}$$

where α is the displacement regulation parameter.

Substituting Eq. 10 into Eq. 9, R becomes:

$$R = \frac{1}{\alpha_{1\min}\alpha_{2\min}} \frac{\eta_{v1,B}\eta_{v2,B}}{\eta_{v1,A}\eta_{v2,A}} \cong \frac{1}{\alpha_{1\min}\alpha_{2\min}} \tag{11}$$

For the usual values of α (~0.3-1), Eq. 11 shows that:
if R < ~3 regulation only concerns the pump;
if ~3 < R < ~9 regulation concerns the pump and the motor.

The motor displacement can be determined by means of the corner power (Eq. 5):

$$P_c = \frac{F_{\max} v_{\max}}{\eta_{g2}} = \frac{V_{2\max}\Delta p_{\max}\eta_{hm2}}{2\pi}\omega_{2\max} \tag{12}$$

Properly taking the value of Δp_{max} and η_{hm2} the motor displacement can be calculated by:

$$V_{2\max} = \frac{2\pi \quad F_{\max} v_{\max}}{\omega_{2\max}\Delta p_{\max}\eta_{hm2}\eta_{g2}} \tag{13}$$

The pump displacement can be calculated by means of a flow rate balance at the intermediate point, i.e. where the pump and motor reach their maximum displacements (Fig. 5):

$$\frac{V_{1\max}\omega_1}{2\pi}\eta_{v1i} = \frac{V_{2\max}\omega_{2i}}{2\pi\,\eta_{v2i}} \tag{14}$$

The intermediate speed ω_{2i} can be determined by dividing the conversion range into two same ratio parts:

$$\omega_{2i} = \omega_{2max} \big/ \sqrt{R} \tag{15}$$

or it can be set in such a way the vehicle speed is equal to the most frequent velocity $\bar{v}$:

1 The usual definition of R, i.e. the corner power divided by the maximum power to the pump, is here substituted for convenience reasons with the given definition.

$$\omega_{2i} = \frac{\overline{v}}{r} i_g \tag{16}$$

Therefore the pump displacement is expressed as:

$$V_{1max} = V_{2max} \frac{\omega_{2i}}{\omega_l \eta_{v1i} \eta_{v2i}} \tag{17}$$

2.4 The Storage Battery

The reference type battery for traction applications is a Lead-acid battery. Ni-Cd batteries are also available on the market, even if in the near future they could be forbidden by the European Union because of their toxicity. A promising solution seems to be the Nickel/metal hydride battery, since it has a high specific energy and should lead to fewer recycling and disposal problems.

Many battery systems are available or under experimentation at present, their main characteristics of which are summarized in Table 1 (Rand et al., 1998; Iqbal, 2003; Miller, 2004; Jefferson et al., 2002), where:

e_s is the energy accumulated by the battery per unit mass;

P' is the maximum power per unit mass that the battery can supply for very short times and is greater than the continuous power;

η_B, the efficiency of the battery, is the ratio between the energy supplied by the battery during the discharge period and the energy supplied to the battery during the charge period providing the initial and final state of charge (SoC) are the same.

$$\eta_B = \frac{\int_{t=0}^{t=t_d} I_d V_d dt}{\int_{t=0}^{t=t_{ch}} I_{ch} V_{ch} dt} \tag{18}$$

where I and V are the current and the voltage respectively; the cycle life is the number of charge cycles before battery degradation, attained when the specific energy of the battery is reduced by 20%.

The battery size can be calculated taking into account the energy accumulation capacity E_c required by the "only electric" operation of the vehicle. So the mass and peak power of the battery are:

$$m_B = \frac{E_c}{e_s}; \; P_{Bp} = P' \; m_B \tag{19, 20}$$

The latter should be greater than the peak power of the EM driven by the battery.

2.5 The Control System

The hydrostatic hybrid system must be supervised by a control system in order to perform the following actions:

- regulation of the vehicle's speed according to the what the driver wants to do;
- regulation of acceleration to avoid exceeding the maximum engine power;
- regulation of decelerations to avoid the electric generator overloading the battery.

Table 1: Status of battery systems in competition with lead/acid batteries for electric vehicles

System	Specific energy e_s [Wh/kg]	Specific peak power P' [W/kg]	Energy efficiency η_B [%]	Cycle life	Self discharge % per 48 h	Cost US$/kWh
Acidic aqueous solution						
Lead-acid	30-50	150-400	60-80	500-1000	0.6	120-150
Alkaline aqueous solution						
Nickel-cadmium	40-60	80-150	75	800	1	250-350
Nickel-iron	50-60	80-150	65	1500-2000	3	200-400
Nickel-zinc	55-75	170-260	70	300	1.6	100-300
Nickel-metal hydride	70-95	200-300	70-75	750-1200	6	200-350
Aluminum-air	200-300	160	< 50	Not available	Not available	Not available
Iron-air	80-120	90	60	500	Not available	50
Zinc-air	100-220	30-80	60	600	Not available	90-120
Flow						
Zinc-bromine	70-85	90-110	65-75	500-2000	Not available	200-250
Vanadium redox	20-30	110	75-85	-	-	400-450
Molten salt						
Sodium-sulfur	150-240	230	85	800	0	250-450
Sodium-nickel chloride	90-120	130-160	80	1200	0	230-345
Lithium-iron sulfide (FeS)	100-130	150-250	80	1000	Not available	110
Organic lithium						
Lithium-ion	80-130	200-300	> 95	1000	0.7	200-300

The first action can be easily performed by operating sequentially on the displacements of the two hydraulic machines: during acceleration, the pump displacement is increased, keeping the motor displacement at its maximum value; then, when the pump displacement reaches its maximum value, the motor displacement is decreased. The opposite occurs during deceleration phases. All these actions must be carried out avoiding the overloads in 2) and 3). This can be done by checking the slip of the electric motor/generator, which, around the synchronous speed, is proportional to the torque. In this way, during acceleration, the slip increases with vehicle load until it reaches its maximum value; in that moment the displacement variation must be stopped so that no further torque increase can be imposed to the EM.

When the vehicle must slow down, i.e. when the drivers takes his foot away from the accelerator pedal, the control system, instead of applying the service brakes, increases the hydraulic motor displacement or reduces the hydraulic pump displacement; in both cases the pressure in the circuit and the motor torque fall so that the vehicle inertia force acts on the hydraulic motor axle reversing the motor function, reversing the high pressure side of the circuit. Consequently, the pump reverses its function too, forcing the electric motor/generator to go past the synchronous speed and become a generator, which will in turn charge the battery. In this way the kinetic energy of the vehicle can be partly recovered.

The hazard of the current peaks can be avoided by again checking the slip: when the electric machine is driven by the pump the slip becomes negative until it reaches its minimum value; at this point the displacement variation must be limited so no further torque will be imposed to the EM and no further current produced. At the same time, the traditional braking system must act to absorb the remaining part of the torque required by the vehicle braking. This is a series regenerative brake system (Miller, 2004), which introduces the electrical regeneration simultaneously with the service brakes in proportion to the pedal position.

The control system suitable for these tasks is a unified command type control (SiDac) (Paoluzzi et al., 1987): only one signal is needed to control the variation of the hydraulic units' displacements and modulation of the braking system. A separate control system will check the charge level of the battery, arranging for the thermal engine to be set on a lower power level when the battery is nearly full.

Particular attention must be paid to ICE management. In order to obtain minimum emission levels, the ICE should be kept in operation even during idle times and braking: it is known, in fact, that during transients the emissions, particularly the particulate matter, increase. Following this criterion, the power coming from the ICE limits the recoverable power during regenerative braking, since the EM can manage a limited power. An alternative criterion is to shut fuel injection off. However, in the on-road drive cycle studied, strong braking, which produces high power at the EM, seldom occurs; what is more frequent is the slowing down caused by traffic, in which the conventional brake isn't used. One can wonder if it is worth cutting off the engine every time slowing down occurs or if it is more convenient to keep the engine always on; all the more so as the battery must be replenished since the vehicle is intended as a charge sustaining parallel hybrid.

This ambiguity should be resolved by careful simulation, or by experimentation.

2.6 Propulsion System Efficiency

The definition of the propulsion system efficiency as a ratio between the energy for the traction and the fuel energy during a defined operation period

$$\eta = \frac{E_{\mathrm{trac}}}{E_{\mathrm{f}}} \tag{21}$$

is not always correct. This is because it doesn't take into account the energy contribution of the battery E_{B}, which is positive when, in the operating period, the energy coming from the ICE is less than the energy required by traction (hypogeneration), or negative in the opposite case (hypergeneration). Therefore, a new rate must be defined. Here, the intrinsic efficiency of the propulsion system during the considered time period was introduced. This can be defined as the ratio between the traction energy E_{trac} and the sum of the energies E_{f} and E_{fb}, i.e. the fuel energy input in the ICE and the fuel energy required by the ICE to bring the battery back to the same initial state of charge. In the case of hypergeneration, E_{fb} is the quota of fuel energy which has been burned in the thermal engine and then stored in the battery as surplus energy E_{B}. Therefore:

$$\eta_{\mathrm{I}} = \frac{E_{\mathrm{trac}}}{E_{\mathrm{f}} \pm E_{\mathrm{fb}}} \tag{22}$$

The + sign refers to hypogeneration, the – sign to hypergeneration.

For both cases, E_{fb} is equal to (see Fig. 3):

$$E_{\mathrm{fb}} = \frac{E_{\mathrm{B}}}{\eta_{\mathrm{B,ch}}\eta_{\mathrm{INV}}\eta_{\mathrm{EM}}\eta_{\mathrm{gI}}\eta_{\mathrm{ICE}}} \tag{23}$$

The same consideration holds for the fuel economy of the vehicle. The *fe* must be substituted by the intrinsic fuel economy fe_{I}, which is the ratio between the distance d and the sum of fuel volume input in the ICE, V_{f}, and V_{fb}. In the case of hypogeneration, V_{fb} is the fuel volume required by the ICE to restore E_{B}: so it must be added to the fuel volume input in the ICE; in the case of hypergeneration, V_{fb} is the quota of fuel which has been burned in the engine during the operating period to store in the battery the surplus energy E_{B}: so, it must be subtracted from V_{f}.

$$fe_{\mathrm{I}} = \frac{d}{V_{\mathrm{f}} \pm V_{\mathrm{fb}}} \tag{24}$$

The intrinsic efficiency and intrinsic *fe* are linked together by the following relation:

$$fe_{\mathrm{I}} = \frac{d \quad \rho_{\mathrm{f}} \quad H_{\mathrm{u}}}{E_{\mathrm{trac}}}\eta_{\mathrm{I}} \tag{25}$$

3 Application to an Urban Bus

A 12 m urban public transportation was chosen for the application of the hydrostatic hybrid system. A hybrid bus, called Ternibus in this paper, (Conti et al., 2000, Jefferson et al., 2002)) was taken as a reference case. The fundamental characteristics were kept, in view of a subsequent comparison of performance and pollutants; they were:

- the target power of the ICE: 30 kW;
- battery electric energy capacity: 70 kWh;
- maximum road grade: 16%.

According to Italian law, the urban bus must reach at least a speed of 60 km/h at full load, and have a power/mass rate of at least 8 kW/t. This second condition makes it possible to calculate the minimum power of the hybrid engine starting from the full load mass of the vehicle. Since the mass is heavily influenced by the size of some components, the onboard power of the vehicle was defined using an iterative process. Thanks to the HHS, the mass of the empty bus was limited to 10 t with 120 kW of onboard maximum power (12 kW/t), i.e. nearly the same mass as in traditional buses with diesel engines in spite of the heavy weight of the storage batteries.

The calculation of the hybrid engine components will be now illustrated.

3.1 Internal Combustion Engine

The ICE power was calculated on the basis of the measured data for buses of the same category: $\bar{v}$ = 15 km/h; c_s = 270 gr/kWh; *fe* = 1.8 km/l; ρ = 0.83 kg/l. With these values Eq. 2 gives $\bar{P}_{req}$ = 25.6 kW, ≈30 kW.

The internal combustion engine chosen was a turbodiesel, direct injection OM660 – by Mercedes (the same used on the commercial car SMART cdi), whose characteristics and performance are reported in Table 2 and in Fig. 6. This engine can supply the required power of 30 kW with a mass of only 65 kg; Fig. 7 shows the emissions produced by this engine according to the 13 mode test of EEC 93/116 directive: their values are all below the EURO3 limits now in force in Europe.

Table 2: Internal Combustion Engine characteristics

Turbocharged diesel engine *OM 660*	
Configuration	3 line cylinders
Displacement, Bore/stroke	799 cm^3, 65.5x79 mm
Compression ratio	18.5:1
Turbocharging pressure	1.15 bar
Injection	Direct injection Common rail
Emission reduction	Three way catalytic cartridge EU3
Volume and mass	800x500x600 mm / 65 kg

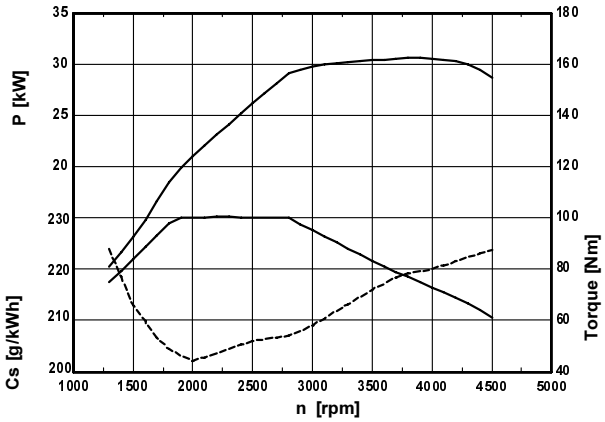

Fig. 6: *Characteristic curves of the internal combustion engine*

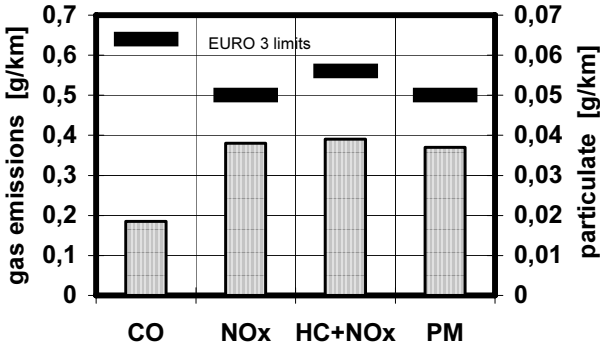

Fig. 7: *Emissions of the ICE according to EEC 93/116 test*

The ICE speed can be chosen inside the range where specific consumption is low, satisfying the power requirement: in Fig. 6 this condition occurs at the speed of 3000 rpm with a specific consumption of 210 gr/kWh. The speed of the EM is the same as that of the ICE because it is possible to modify it by changing the frequency.

3.2 Electric Motor and Inverter

The electric motor was a commercial unit that provides 60 kW/90 kW nominal/peak power, with a synchronous speed of 3000 rpm, and maximum slip of about 4%; its efficiency ranges from 89 to 92%. In Fig. 8, the torque of the EM as a function of the slip is shown. The characteristics of the EM and the inverter are reported in Table 3.

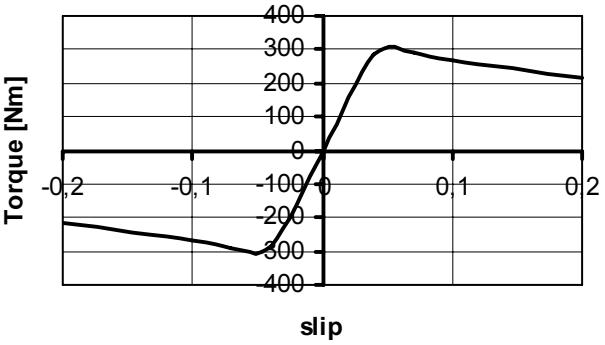

Fig. 8: *Electric motor: curve of torque vs slip*

Table 3: Characteristics of the drive system

General Charcteristics	Type	Alternate current drive system	
	Battery voltage	240 V	
	Operating temperature	-20 ÷ 65°C	
	Cooling	Water-glycol	
Electric Motor		**Inverter**	
Type	Permanent magnets	Type	IGBT
Phases / poles	3 / 8	Voltage range	180-400 V
Design /max torque	150/215 Nm	Battery max current	550 A
Constant torque range	0-4000 rpm	max alternating current	800 A
Constant power range	4000-10000 rpm	Control method	Field attenuation
Maximum speed	12000 rpm	Max frequency	800 Hz
Continuous/peak power	60/90 kW	Switching frequency	4kHz
Dimensions, mass	250x230 mm, 58 kg	Dimensions, mass	360x320x135mm, 30 kg

3.3 Storage Battery

As previously discussed, the NiMH technology seems to be the most suitable solution, having a specific energy nearly double that of a traditional Pb-acid battery and the highest peak power among the available solutions. The cost of a NiMH battery is higher: the investment costs would be balanced by the lower operating cost due to the lower mass the vehicle has to move. A long term simulation of the vehicle and an investment analysis would have to be carried out in order to verify the effectiveness of this choice. The Lithium-ion battery could be a good alternative to the NiMH battery because it offers higher efficiency and higher energy density (see Table 1), but it is not yet available for these applications.

For buses and trucks modules of NiMH batteries of high specific energy (75 Wh/kg, specific power 160 W/kg) are available. Remembering that the required energy accumulation capacity must be equal to 70 kWh, the mass and the peak power of the battery are respectively 933 kg and 149 kW (Eq. 19 and 20). The latter quantity is greater than the 90 kW of peak power produced by the electric motor working as a generator; hence, the risk of overload of the batteries seems to be low. Assuming a depth of discharge equal to 50%, the "only electric" period allowed by this battery to the vehicle in examination at full load and at an average speed of 15 km/h exceeds 2 hours.

3.4 Hydrostatic Transmission

To determine the size of the hydrostatic transmission, the following quantities have to be calculated (Paoluzzi et al., 1983; Scuto and Leone, 1983; Tramontan, 2001):

maximum drive power P: the sum of the ICE power and EM power: 30 kW+90 kW =120 kW

vehicle mass m_v: this value was calculated adding the weight of the reference bus without the engine, 8520 kg, to the mass of the components of this hybrid engine, resulting in 9906 kg. With 71 passengers, a usual number for this vehicle category, having each an average mass of 70 kg, the vehicle mass at full load condition is equal to 14876 kg, rounded to 15 t. Therefore, the power-mass ratio is equal to 120/15 kW/t =8 kW/t, as recommended by Italian law.

wheel radius r: using the tyre type 315/80 R22,5 the radius is r = 0,538 m

final drive ratio i_g: as in reference bus i_g=8

load on the traction axle F_A: the weight on the posterior axis is nearly 60% of the total weight, so F_A= 88200 N

3.4.1 Maximum Resistance Force

The resistance force the vehicle must overcome is composed of aerodynamic force, rolling resistance force and weight force due to road grade and the adherence limit must also be verified. The calculations are summarized in Table 4, where the numerical values have been derived from the reference bus.

Table 4: Resistance force calculation

Aerodynamic force $F_a = \frac{1}{2}\rho_a c_D v^2 A$ =1270 N	v=16.7 m/s A=2.09x3.09=6.46 m^2 c_D=1.16 ρ_a=1.21 kg/m^3
Rolling resistance force $F_R = f m_v g$ = 2790 N	f=0.019 m_v=15000 kg
Road grade force $F_G = m_v g \sin\beta$ = 23230 N	grade 16% → β=9.1°
Maximum resistance force $F_{max}=F_a+F_R+F_G$=27290 N	
Maximum tractive force $F_H = \mu F_A$ = 70560 N ≥ F_{max}	F_A =88200 N μ = 0.8

3.4.2 Hydrostatic Transmission Design

For the conversion range calculation (Eq. 9), only the power of the EM, 90 kW, can be considered as P_{he}, since the vehicle could be required to work in only electric operation for long periods. Assuming as average values η_{g1} = 0.94, η_{g2} = 0.92, η_{ht} = 0.78, Eq. 9 gives R = 7.45. Since R > 3 the displacement regulation must be adopted for both the pump and motor of the HT.

The pump and motor displacements can be calculated from Eq. 13 and Eq. 17 carefully choosing appropriate values for the efficiencies and the maximum

operating pressure. Economic considerations suggest using high specific power motors so the operating pressure must be the maximum available for this type of application.

The pump speed cannot be set equal to the speed of the motors since the most suitable pumps for this application (piston pumps) don't reach the speed of 3000 rpm unless their displacements are small; therefore, a gear box to lower the speed would seem to be necessary. However, a speed higher than the maximum speed recommended by the builder could still be adopted if a shorter life of the pump is accepted (the pump isn't the component in a hybrid engine that has the shortest life), making it possible to avoid having to use a gear box. For the case at hand, the flow rate requirements can be satisfied at n=3000 rpm by a pump with 125 cm^3/rev, even if its recommended maximum speed is 2850 rpm.

The motor and pump displacement calculation are summarized in Table 5. A swashplate axial piston pump and a bent-axis axial piston motor were chosen from a commercial catalogue; their characteristics are shown in Table 6.

Table 5: Motor and pump displacement calculation

Motor displacement $V_{2\max} = \frac{2\pi \quad F_{\max} v_{\max}}{\omega_{2\max} \Delta p_{\max} \eta_{\text{hm2}} \eta_{\text{g2}}}$ $V_{2\max}$=341 cm^3/rev	$F_{\max}$=27290 N $\Delta p_{\max}$=400 bar $v_{\max}$=16.7 m/s η_{g2}=0.92; η_{hm2}=0.92 $\omega_{2\max} = \frac{v_{\max} i_{\text{g}}}{r}$ = 248 rad/s
Pump displacement $V_{1\max} = V_{2\max} \frac{\omega_{2\text{i}}}{\omega_1 \eta_{\text{v1i}} \eta_{\text{v2i}}}$ $V_{1\max}$=119 cm^3/rev	$\omega_{2\text{i}} = \frac{\omega_{2\max}}{\sqrt{R}}$ =91 rad/s ω_1=314 rad/s η_{v1i}=0.91 η_{v2i}=0.91 R=7.45

Table 6: Pump and motor characteristic data

		PUMP	MOTOR
$V_{\max}$	cm^3/rev	125	355
$n_{\max}$	rpm	2850	2950
$\Delta p_{\max}$	bar	400	450
mass	kg	80	170
Moment of Inertia	kgm^2	0,023	0,102

4 System Simulation

In order to evaluate the functional characteristics of the system and to compare its performance and efficiency with those of similar solutions, a simulation model of HHS was developed using ITIsim, a program for the dynamic simulation of fluid power and mechanical systems (ITI Sim 3.3, 2003).

4.1 The Model

The system being analyzed is made up of the propulsion group (the ICE, EM, battery and inverter), HT, control system, braking system and loads. Each component of the system was described by a built-in model of the code or by "ad hoc" models.

The scheme of the system model is reported in Fig. 9 and made up of the following components.

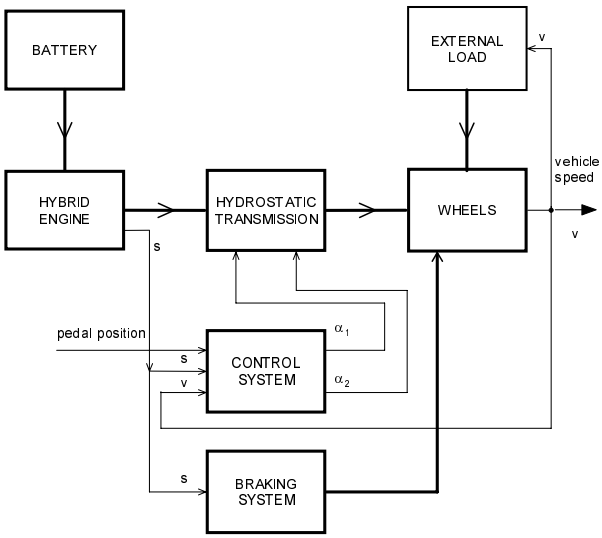

Fig. 9: *Full model of the propulsion group*

The *hybrid engine* which simulates the operation of the ICE using the characteristic curve in Fig. 6 and the operation of the EM using the curve in Fig. 8 and an average efficiency η_{EM}=0.9.

The *battery* which simulates the battery and the inverter operation by means of the efficiency, respectively η_{B}=0.7 and η_{INV} = 0.95.

The *hydrostatic transmission* which reproduces the characteristics of a closed circuit HT having the regulation on both the hydraulic pump and motor. The model makes it possible to take into account the hydromechanical and volumetric losses: the former are modeled by means of the Stribeck curve which also includes pressure and speed dependency; the latter are modeled by a simple conductance (loss proportional to the pressure drop). The constants of these loss models were adjusted to better approximate the efficiencies of the two real machines. In Fig. 10 the pump efficiencies resulting from the loss models are shown; similar curves can be found for the motor.

The *external load* which models the road grade force, rolling resistance force, aerodynamic force and inertia force. All these forces and inertias are transferred to the wheel axle. The final drive is described by its ratio i_{g} and a constant efficiency η_{g2} =0.92.

The *control and braking systems* which, following a strategy dependent on vehicle speed and load, generates a suitable signal acting on the displacements of the two hydraulic units and applies the traditional braking system.

The *energetic accounting subsystem* which calculates the energy, power, and efficiency of the main components as well as the *fe* of the vehicle.

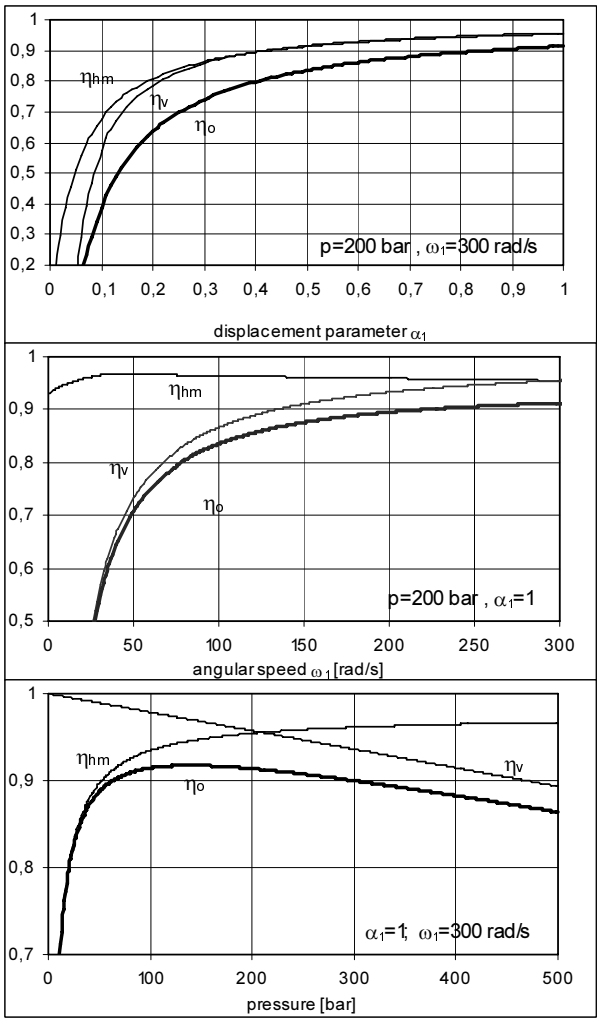

Fig. 10: *Pump efficiencies as function of speed, displacement and pressure difference*

4.2 The Control System

The control system was only studied to satisfy the requirements of the simulation, hence, without the complexity and completeness of a conventional control system for hydrostatic transmission.

The control system must regulate the vehicle speed and supervise the power level of the EM.

The first function can be carried out using a proportional-integral controller acting on the displacements (Fig. 11).

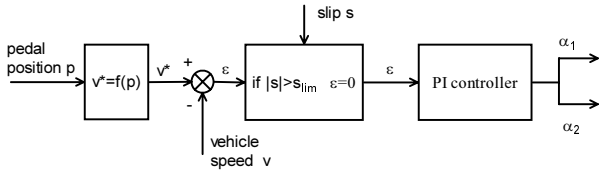

Fig. 11: *Scheme of the control system*

The desired speed v^* is set by the accelerator pedal position (or equivalent command) and compared with the vehicle speed v; the consequent error ε enters the PI controller to generate the new displacements for the pump and motor and hence the new vehicle speed. This process develops sequentially on the pump and motor displacements, as explained in section 2.5.

During these actions, the control system sets a limit to the power of the EM by means of the control variable s, the motor slip, which is directly linked to the torque of the EM (Fig. 8): when s exceeds the maximum value, for example during acceleration, the error ε is set equal to zero and the controller stops changing the displacements. During decelerations, the control system applies the traditional braking system only when s reaches the minimum value for the generator operation; in this way the vehicle can decelerate in any way exploiting the maximum power of the generator without overloading the storage battery.

5 Performance Estimation

An estimation of the vehicle's performance can be made by comparing and matching the tractive force curve of the engine with the road load curve.

The tractive force curve represents the maximum force that the propulsion group can supply when varying the vehicle's speed. It can be drawn by transforming the characteristic curve of the HT $M_2=f(\omega_2)$ into the curve $F=f(v)$ by means of the following relations:

$$F = \frac{M_2 \eta_{g2} i_g}{r} \; ; \; v = r \frac{\omega_2}{i_g} \qquad (26, 27)$$

In the plot of Fig. 12, the tractive force of the vehicle is matched with the road load for the 0% grade and for 16% grade. Two power levels are superimposed on the plot: full power and "only electric". The intersections of the tractive force with the road load determines the top speed on the grade: on level grade the top speed is nearly 65 km/h, 5 km/h over the legal limit. In "only electric" mode, the vehicle can reach 56 km/h and is able to start on a road with a 16% grade keeping a constant speed of 6 km/h.

In Fig. 13 the acceleration curves for level grade and 16% grade at full passenger load are reported. The hydrostatic transmission efficiency is also presented: it shows low values during the first seconds after starting, because of the intervention of the relief valves and because of the small values of the pump displacement. It can be noticed that the maximum HT efficiency occurs for speed values around 20 km/h, which is the average speed registered in urban areas.

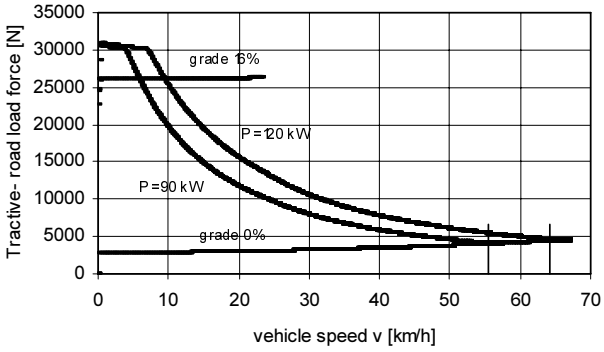

Fig. 12: *Tractive and road load force matching at maximum load (m_v=15000 kg)*

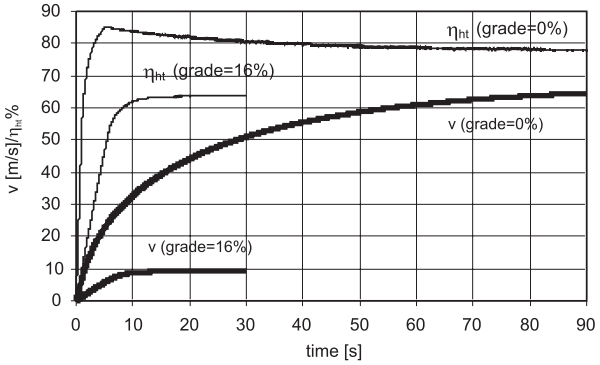

Fig. 13: *Vehicle acceleration performance for level grade and 16% grade, and hydrostatic transmission efficiency at maximum load (m_v=15000 kg)*

5.1 Simulation of Standard Cycles

Two standard driving cycles were selected for use in this short test. The first one is the standard cycle CBD-14 (O'Keefe et al., 2002), which is able to capture the stop-and-go nature of a typical bus duty cycle: maximum speed of 32 km/h and duration of 40 sec to be repeated 14 times. The second standard cycle is the driving cycle SAE J227a (Iqbal, 2003), recommended by the Society of Automotive Engineers to evaluate the performance of electric vehicles. It has three schedules designed to simulate the typical driving patterns of a fixed route urban (schedule B), variable-route urban (C) and variable-route suburban (D) travels. Here a simplified version of the first two schedules were used. The selected cycles are reported in Fig. 14.

In the analysis, two ICE regulation criteria were considered: in the first one, during braking and idle times the ICE is idling, in the second the ICE is always in operation.

The bus was assumed to be used at full load (71 passengers, equivalent to a vehicle mass of 15 t) on level grade. A constant power drain from the battery equal to 2,5 kW was considered to account for the ancillary loads. Some results of the simulations are reported in Table 7.

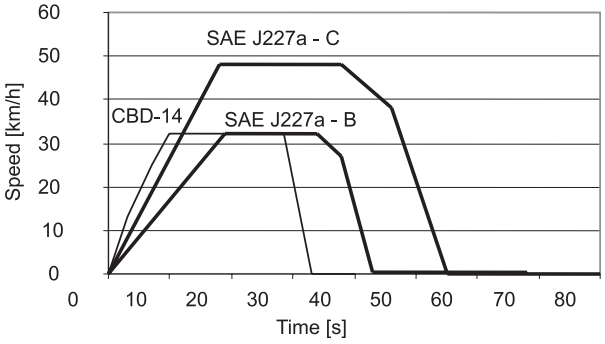

Fig. 14: *Standard driving cycles. CBD-14: maximum speed 32 km/h, time cycle 40 s, 14 cycles. SAE J227a-Schedule B: maximum speed 32 km/h, time cycle 68 s, 5 cycles; Schedule C: maximum speed 48 km/h time cycle 80s, 3 cycles*

Table 7: Performance of the system for the selected standard cycles

	CBD-14	SAEJ227a B	SAEJ227a C
n.	14 cycles	5 cycles	3 cycles
total time	560 s	340 s	240 s
distance	3.29 km	1.34 km	1.56 km
	Engine idling / on	Engine idling / on	Engine idling / on
η_l	0.204/ 0.202	0.193 /0.224	0.2/ 0.213
η	0.443/ 0.319	0.39 / 0.19	0.727 / 0.35
fe_l [km/l]	1.87 / 1.83	1.98/ 2.3	1.85/ 1.97
fe [km/l]	4.05 / 2.89	3.87 / 1.94	6.72 / 3.19
E_{trac} [kJ]	13197	4806	6198
E_{ICE} [kJ]	11715/16800	5100 / 10200	3420 / 7200
E_B [kJ]	10068/ 7078	3545/ -1123	6485/ 3227
SoC [%] Initial value 80%	76/ 77.2 hypo /hypo	78.6/ 80.4 hypo /hyper	77.4/ 78.7 hypo /hypo

In almost all the driving cycles the propulsion system works in hypogeneration condition, so the values of the efficiency η and fe appear to be completely unreal. However, if the energy required for replenishing the battery (Eq. 23) is also considered, the intrinsic efficiency and the intrinsic fe assume more correct values: the fe_l varies from 1.8 to 2.3, whereas the average fe of traditional diesel buses ranges from 1.5 to 1.8 km/l.

O'Keefe et al. (2002) showed a fe equal to 1.36 km/l for a 12 m diesel bus similar but not equal to the one studied here under the CBD-14 cycle and with all auxiliary loads on (the main one is the air conditioner). For a series hybrid bus under the same conditions, they show 1.41 km/l; if the air conditioner is off, the fe rises to 1.7 and 1,81 km/l respectively.

In regards to the regulation criteria of the ICE, Table 7 shows that, when the idle times are short (as in the CBD-14 cycle), it is better to let the engine idle; on the other hand, when idle times are long, as in SAEJ227a cycles, the fuel burned just to keep the engine idling weighs on the energy balance, as shown by the values of the intrinsic efficiency in Table 7. Furthermore, for the first regulation criterion (idling), the SoC drops so quickly that a continuous operation of 8 hours cannot be assured. For these reasons the more advantageous criterion seems to be the second one.

In Fig. 15 some significant quantities during the first cycle of schedule C are shown. In particular, starting from the time of 10 sec, the vehicle speed moves away from the target speed: the slip reaches the maximum value (s=0.04) and the control system limits the required power acting on the motor displacement. During the start up, where the tractive power is greater than ICE power, the battery supplies the difference, as shown in Fig. 15 by the SoC decrease; during regenerative braking (38 s < t < 55 s) the pressure difference inverts its direction so the slip becomes negative and the motor acts as a generator charging the battery. The

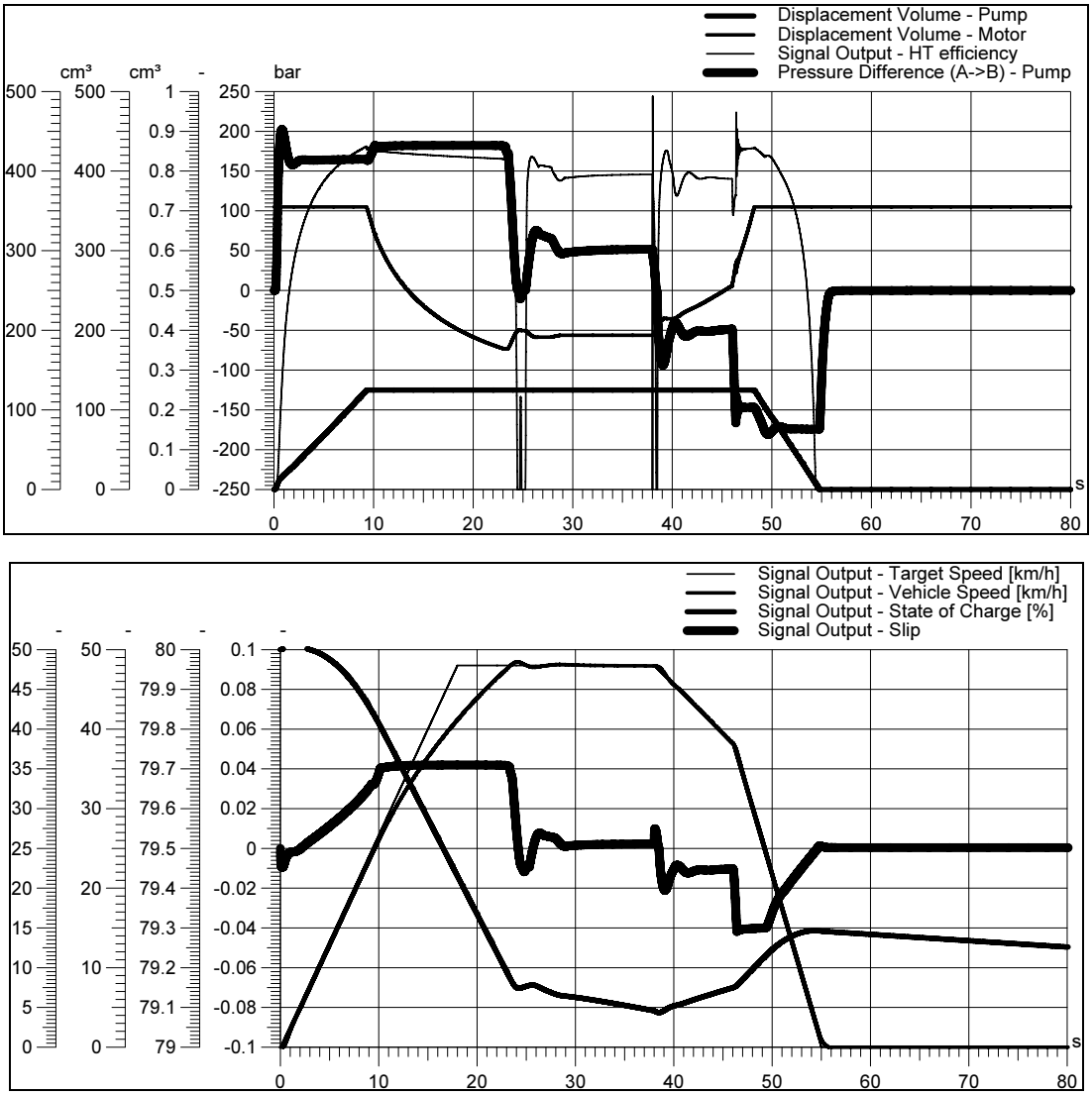

Fig. 15: *SAE J227a C (engine off): Trends of some significant quantities during the first cycle*

SoC increase shows that the accumulated energy in the battery during the regenerative braking (435 kJ) is 33% of the vehicle's kinetic energy (1333 kJ). However, subtracting the energy losses due to the rolling resistance (211 kJ) and aerodynamic load (55 kJ) from the kinetic energy, and adding the power drain from the battery for auxiliaries (43 kJ) to the accumulated energy, the quota of kinetic energy recovered increases up to 45%.

6 Comparison with the Reference Case

In this section, the comparison of performance and emissions of the proposed hybrid solution and the reference solution will be shown.

The only difference between the two buses is in the hybrid units, since the remaining parts, chassis and body, can be considered unchanged. Therefore, the characteristics of the engine in the bus with the hydrostatic hybrid system (HTbus) and the one in the reference bus (Ternibus) are summarized as follows:

HTbus: parallel hybrid engine with hydrostatic transmission; ICE 30 kW-EURO3; EM 60/90 kW at 3000 rpm; battery NiMH, 70 kWh; v_{max} = 60 km/h.

Ternibus: series hybrid engine; EM for traction 128/164 kW at 1500 rpm; ICE (EURO2)+electric generator 30 kW; battery Pb-acid, 70 kWh; v_{max} = 60 km/h.

The masses and volumes of the two hybrid engines are compared in Table 8. The HTbus is approximately 2000 kg lighter, mainly due to the reduced mass of the battery and the lack of an electric generator.

Table 8: Comparison of masses and volumes for the two vehicles

	HTbus		**Ternibus**	
	Mass [kg]	Volume [m^3]	Mass [kg]	Volume [m^3]
ICE	65	0.24	270	0.8
EM	113	0.046	485	0.105
EG			500	0.1
Inverter	30	0.016	80	0.143
Battery	933	1	2000	2
battery charger			110	0.13
HT	300	0.2		
Total	~1441	~1.5	~3445	~3.3

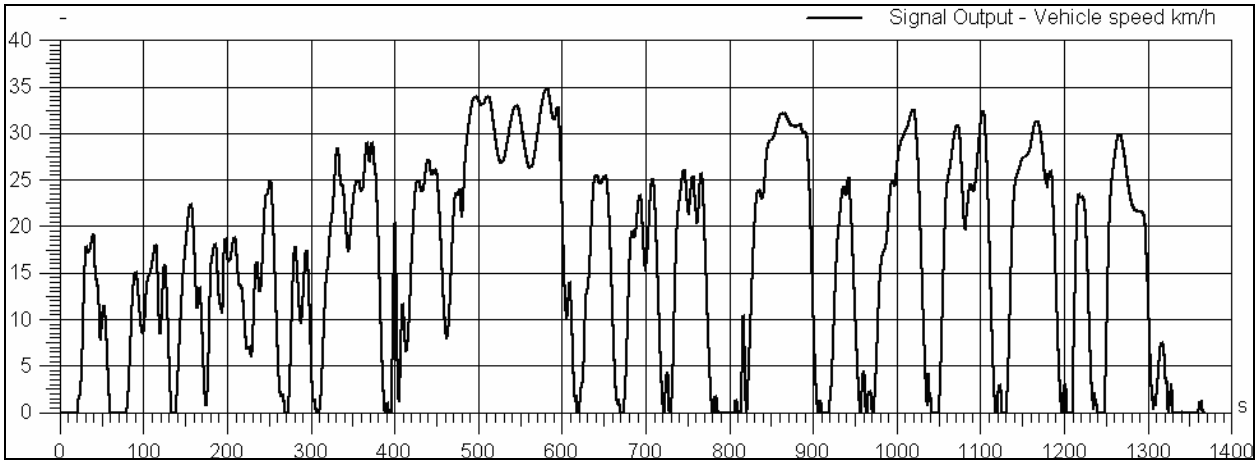

Fig. 16: *Drive cycle of Mission 3 22.06.99*

The performance and emissions were compared on the basis of a test run of Ternibus, carried out during the FLEETS project (Conti et al., 2000) called Mission 3-22-6-99. The drive cycle of the mission is shown in Fig. 16: it represents a typical driving pattern in densely populated urban areas. The measured data are shown in Table 9. The simulation of the mission was carried out assuming the same boundary conditions for the HTbus: distance, driving cycle, road grade. The vehicle mass and passenger mass were respectively 10000 kg and 2100 kg. The vehicle ancillary and accessory load was taken into account by a fixed power drain from the battery equal to the one registered on Ternibus during the mission.

In Table 10 the results of the simulation of the mission are reported.

Table 9: Measured data of Mission 3-22-6-99

Distance	km	5.96
Total time	s	1382
Electric operation time	s	60
Measured Diesel oil consumption	l	2.35
Energy released by battery (at terminals)	kWh	3.61
Diesel oil consumption for replenishing the battery*	l	1.65
Energy for vehicle ancillary and accessory loads	kWh	1.01
Vehicle mass	kg	12100
Average mass of passengers (30 x70 kg)	kg	2100
Road grade	%	0

* this value was estimated by Conti et al. (2000) on the basis of the same criterion used in paragraph 2.6.

The intrinsic fuel economy fe_I and intrinsic efficiency η_I of the HTbus are higher than those of Ternibus: this is mainly due to a lower vehicle mass (~2 t), which decreases the inertia forces and rolling resistance forces, and to the higher ICE efficiency. As a comparison, the average *fe* recorded by Conti et al. (2000) over the whole test were: *fe* =2.27 km/l and fe_I =2.43 km/l; during the same experimentation a traditional diesel bus, on the same routes in almost the same traffic conditions, showed *fe*=2.28 km/l.

The engine idling during braking and idle times does not seem to be advantageous, as shown by fe_I in Table 10. What's more, since the final SoC is very low, a decrease equal to 3.4 % in 23 minutes leads to a lower limit of the charge, 40%, in only 6 hours. In this case as well a long operation period does not seem to be guaranteed.

Table 10: Comparison of performance

	HTbus		Ternibus
Mission 3-22.06.99	total time 1382 s distance 5.96 km		
	idling engine	engine on	
η_I	0.175	0.226	0,212*
η	0.278	0.137	0,361*
fe_I [km/l]	2.74	3.51	1.49
fe [km/l]	4.35	2.13	2.54
E_{trac} [kJ]	14085	14085	Not measured
E_{ICE} [kJ]	20280	41460	Not measured
E_B [kJ]	8577	-11756	12996
SoC [%] (Initial value 80%)	76.6 hypogen.	84.7 hypergen.	74.2 hypogen.

*estimated values

The high final SoC of the second criterion suggests an alternative strategy: the regulation of the engine load by means of a control system, which keeps the SoC between fixed limits. In this way the double energy conversion in the battery could be reduced, and the ICE could have a longer life.

In Table 11, the emissions of the two buses and a traditional diesel bus are compared. The emissions of HTbus were evaluated using the model on the basis of the measured data, according to the variable speed test of EEC 93/116 directive (Fig. 7), whereas the ICE in this scheme works at a constant speed. This probably leads to lower emissions with respect to the calculated ones, especially for particulates. Even though the comparison involves simulated and measured data, it is evident that the HTbus emissions are definitely lower than the European EURO3 limits and very close to EURO4 limits.

Table 11: Comparison of emissions

Emissions [g/km]	HTbus	Ternibus	Diesel bus	EU3/EU4 Limits
CO	0.18	0.30	5.05	0.64/0.5
NO_X	0.37	11.55	24.92	0.5/0.25
$HC+NO_X$	0.39	12.14	25.74	0.56/0.3

7 Conclusions

A hydrostatic hybrid system for vehicular propulsion was presented. An internal combustion engine is coupled with an electric asynchronous machine, which gives or receives energy from a battery according to the torque required by the traction. A hydrostatic transmission distributes the power to the wheels by continuously varying their speed; its flexibility allows the thermal engine to run at constant speed, i.e. at the maximum efficiency and/or minimum emission conditions, and the electric generator to recharge the battery without dangerous current peaks. This last point allows the designer to adopt a more powerful battery than the traditional and reliable Pb-acid battery, in this way saving on the onboard mass of the vehicle.

The hydrostatic hybrid system presented here has the main positive features of both series and parallel schemes without having the respective drawbacks. In fact, the internal combustion engine works at a fixed point and is sized for the average power, as in a series scheme; both an internal combustion engine and electric motor supply power to the wheels since they are coupled as in a parallel scheme. This makes it possible to reduce the size and mass of the ICE and EM. Regenerative braking increases the efficiency of the vehicle.

A unified command type control system controls the displacements of the hydraulic machines for speed regulation. Moreover, by means of a simple control strategy, it avoids electric overloads on the battery and makes it possible to manage the regenerative braking in an optimal way.

The hydrostatic hybrid system was applied to a "12m" class bus. A hybrid bus, recently used for experiments in Italy, was taken as a reference. The hybrid group was designed referring to current technologies, without preferring more expensive or innovative solutions, although they do exist. In fact, an internal combustion engine, an automotive diesel engine, 800 cc, 30 kW and a compact electric drive system available today were chosen. The NiMH technology was adopted for the battery because it guarantees double specific power with almost the same efficiency as a traditional Pb-acid solution.

The operation of the vehicle was simulated using the reference bus test data as input. The comparison showed a higher efficiency and an emission reduction for the proposed solution.

One problem in particular was not examined here: the issue of noise. In an urban environment, the increased noise of this system might cause problems but prototype testing must be carried out to determine whether or not noise will be a problem.

Nomenclature

A	frontal area of the vehicle	[m^2]
c_D	drag coefficient	/
c_s	specific consumption	[kg/J, g/kWh]
d	distance covered	[m]
E	energy	[J]
f	rolling resistance coefficient	/
F	force	[N]
fe,fe_l	fuel economy, intrinsic fuel economy	[m/m^3, km/l]
H_u	low heat value of the fuel	[J/kg]
i_g	final drive ratio	/
m	mass	[kg]
M	torque	[Nm]
n	rotational speed	[rpm]
P	power	[W]
P_c	corner power	[W]
r	wheel radius	[m]
R	conversion range	/
v	vehicle speed	[m/s, km/h]
V	pump or motor displacement	[m^3/rev, cm^3/rev]
V_f	fuel volume	[m^3]
α	displacement regulation parameter ($V=\alpha V_{max}$)	/
Δp	pressure difference	[Pa, bar]
η, η_l	efficiency, intrinsic efficiency of the propulsion system	/
η_{g1}	efficiency of the speed reducer	/
η_{g2}	efficiency of the final drive	/
η_{hm}	hydromechanical efficiency	/
η_{ht}	efficiency of the hydrostatic transmission	/
η_o	overall efficiency	/
η_v	volumetric efficiency	/
μ	wheel-road friction coefficient	/
ρ_a, ρ_f	air density, fuel density	[kg/m^3]
ω	angular speed	[rad/s]
Subscripts		
B	referred to the battery	
EM	referred to the electric motor	
ICE	referred to the internal combustion engine	
INV	referred to the inverter	
ch, d	Charge, discharge	
f	referred to the fuel	
i	referred to the intermediate point	
p	peak value	
req	required	
trac	traction	
1,2	referred to the hydraulic pump, to the hydraulic motor	

References

Bitsche, O. and **Gutmann, G.** 2004. Systems for Hybrid Cars - Review. *Journal of Power Sources* 127 (2004),), pp 8-15. Elsevier Ltd.

Conti, M., **Leonelli, V.**, **Pallacorda, M.** and **Ragona, R.** 2000. La flotta ibrida a Terni- misure e risultati. (The Hybrid Fleet in Terni - Measurements and Results) *ENEA internal report*.

Gulia, N. and **Yurkov, S.** 2001. Hybrid power units for municipal buses. *Nauka i Tekhnica*,UA 2001.

Huang, K. D. and **Tzeng, S. C.** 2004. A New Parallel-type Hybrid Electric Vehicle. *Applied Energy 79* (2004), pp 51-64. Elsevier Ltd.

Iqbal, H. 2003. *Electric and hybrid vehicles*. CRC Press LLC.

Jefferson, C. M. and **Barnard, R. H.** 2002. *Hybrid Vehicle Propulsion*. WIT Press, London.

Maggetto, G. and **Van Mierlo, J.** 2001. Electric Vehicles, Hybrid Electric Vehicles and Fuel Cell Electric Vehicles: State of the Art and Perspectives. *Ann. Chim. Sci. Mat*, 26(4), pp 9-28. Elsevier, Paris.

Mikeska, D. and **Ivantysynova, M.** 2002. Virtual prototyping of power split drives. *Proc. Bath Workshop on Power Transmission and Motion Control PTMC 2002*, Bath, UK, pp. 95 - 111.

Miller, J. M. 2004. Propulsion Systems for Hybrid Vehicles. *IEE Power and Energy Series 45* - The Institution of Electrical Engineers, London.

Nervegna, N. 2000. *Oleodinamica e Pneumatica*, Vol. 1-3. Politeko, Torino.

Northeast Advanced Vehicle Consortium. 2000. Hybrid-Electric Drive Heavy-Duty Vehicle Testing Project - Final Emissions Report. *Defense Advanced Research Projects Agency Agreement No.*: NAVC1098-PG009837.

O'Keefe, P. M. and **Vertin, K.** 2002. *An Analysis of Hybrid Electric Propulsion Systems for Transit-Buses- Milestone completion report*. National Renewable Energy Laboratory. U.S. Department of Energy. NREL/TP-540-32858

Paoluzzi, R., **Zarotti, G. L.** and **Rigamonti, G.** 1987. *SiDAC architectures in hydrostatic transmission control*. Cemoter-CNR, Ferrara, pubbl. N° 352.

Pini Prato, A. and **Corallo, C.** 2000. Soluzioni tecnologiche alternative per i mezzi di trasporto pubblico: lo stato dell'arte e l'esperienza Altrobus. (Alternative solutions for urban public transport: state of the art and the Altrobus experience) *Meeting: "Inquinamento e traffico nei centri urbani: soluzioni tecniche e prospettive"*. Genova 26 ottobre 2000.

Rand, D. A. J., **Woods, R.** and **Dell, R. M**. 1998. *Batteries for electric vehicles*. Research Studies Press Ltd, Tounton.

Scott Wayne, W., **Clark N. N.**, **Nine, R. D.** and **Elefante, D.** 2004. A comparison Emissions and fuel economy from Hybrid electric and conventional-drive transit buses. *Energy & fuels 18*, pp 257-270.

Tramontan, M., **Macor, A.** and **di Riso, I.** 2002. Trasmissioni oleodinamiche di potenza per veicoli ibridi. (Hydraulic trasmissions for hybrid vehicles). *Oleodinamica e Pneumatica- Tecniche Nuove*, Milano. April 2002.

Alarico Macor
was born in 1956; MSc in Mechanical Engineering, 1981; Ph.D. in Energetics, 1987; currently Associate Professor of "Fluid Machines" at the Department of Management Engineering, University of Padova.
His major field of research are: fluid power, hybrid engines for vehicular propulsion, hydraulic turbomachinery.
Other fields: energy systems, thermoeconomic analysis, biofuels.

Marco Tramontan
was born in 1970; MSc in Mechanical Engineering, 2001; Komatsu Utility Europe – Engineering Division since 2001, currently Research&Test Team Leader.
Technical Advisor at Mechanical Engineer Department, University of Padova 2002–2004.
His major field of activity are: NVH, fluid power, industrial engines.
Other fields: hybrid engines for vehicular propulsion.